Structure and activity of $Pd/V_2O_5/TiO_2$ catalysts in Wacker oxidation of ethylene

Róbert Barthos[*], *András Hegyessy*, *Gyula Novodárszki*, *Zoltán Pászti*, *József Valyon*

Institute of Materials and Environmental Chemistry, Research Centre for Natural Sciences, Hungarian Academy of Sciences, Magyar tudósok körútja 2, Budapest 1117, Hungary

*Corresponding author. Tel:+36 1 3826861

E-mail addresses: barthos.robert@ttk.mta.hu (Róbert Barthos), hegyessy@gmail.com (András Hegyessy), gyula.novodarszki@ttk.mta.hu (Gyula Novodárszki), paszti.zoltan@ttk.mta.hu (Zoltán Pászti), valyon.jozsef@ttk.mta.hu (József Valyon)

Abstract

Studies reveal that V_2O_5 supported on TiO_2 is more active in gas phase oxidation reactions by O_2 than on Al_2O_3 or SiO_2 support. Nevertheless, the $Pd/V_2O_5/TiO_2$ catalyst was hardly studied in heterogeneous Wacker-oxidation. The present study concerns preparation of $Pd/V_2O_5/TiO_2$ catalysts and activity of the catalysts in selective gas phase oxidation of ethylene by O_2 in presence of water at atmospheric pressure and in the temperature range of 100-200 ^oC. The influence of palladium and vanadia loading and the partial pressures of the reactants on the yield of oxidation products (acetaldehyde and acetic acid) were examined. The surface-bound vanadia forms were identified by X-ray diffractometry (XRD), X-ray photoelectron spectroscopy (XPS), and FT-Raman spectroscopy. The best activities were achieved with catalysts, having near to monolayer vanadia coverage of the support. Time-on-stream catalytic tests and chemical analysis of the fresh and used catalysts proved the structural and catalytic stability of the $Pd/V_2O_5/TiO_2$ preparations. It was shown that under the conditions of Wacker-oxidation primary product acetaldehyde could become further oxidized to CO_2, whereas no consecutive oxidation of product acetic acid proceeded.

1. Introduction

The oxidation of ethylene to acetaldehyde by contacting ethylene and oxygen gases with a catalyst system, dissolved in water was first described by Schmidt et al. [1]. The aqueous solution contained $PdCl_2$, and, in higher concentration, $CuCl_2$. The copper and palladium was shown to act together in initiating and maintaining the catalytic oxidation process. In the aldehyde-forming reaction the ethylene reduces Pd^{2+} to Pd^0. The role of Cu^{2+} ions is the *in situ* selective regeneration of Pd^{2+}. The final step of the catalytic cycle is the oxidation of CuCl to $CuCl_2$ by O_2 [2]. It was shown that the rate-controlling step of the process is the third-order reaction between dissolved oxygen and CuCl, which reaction is favoured at very low pH values, i. e., at high HCl concentrations [3]. However, the high chloride concentration leads to formation of undesired chlorinated by-products from olefins, especially from higher olefin reactants. Additional drawbacks of the reaction system are the corrosiveness of the liquid phase reaction medium, formation of noxious copper waste by disproportionation of Cu^+ to Cu^0 and Cu^{2+}, precipitation and aggregation of Pd, leading to Pd loss and, thereby, to extra expenses.

As a matter of fact, heterogeneous catalyst was used when the selective oxidation of olefin to carbonyl compounds was first recognized. Based on these early results a pilot plant was built for carrying out the reaction. Moist ethylene/oxygen mixture was passed through a tube reactor, loaded by solid catalyst. However, deactivation and short lifetime of the catalyst turned attention toward homogeneous, liquid-phase catalyst, which was then exploited in industrial practice [4]. In order to overcome the drawbacks of homogeneous Wacker catalyst system the use of chlorine-free terminal oxidants were suggested to be used in absence or in presence of oxygen using $Fe_2(SO_4)_3$ oxidizing agent [5] or phosphomolybdic acid and benzoquinone as catalyst [6, 7], respectively.

Although Wacker plants using dissolved catalyst system are operating commercially, the intent of realizing heterogeneous catalytic olefin partial oxidation is not diminishing. The solid Wacker-type catalysts, studied up to now, can be classified as (i) microporous materials, (ii) heteropoly compounds, and (iii) supported transition metal oxides [8]. The microporous materials were usually zeolites. In the zeolite Wacker catalyst the negatively charged zeolite framework corresponds to the chloride anions of the common solution catalyst, whereas metals, corresponding to the active redox pair in the solution catalyst (Pd and Cu), balance the framework charge. Espeel et al. [9] found zeolite to be efficient 'solid solvent' and showed that palladium and copper exchanged zeolite Y converts ethylene to acetaldehyde in exactly the same way as homogeneous Wacker catalyst. Other authors [10] reported that Cu,Pd,H-mordenite is active in the Wacker-type oxidation of carbon monoxide. Layered clays also allow for intercalation of metal cations between negatively charged layers. Mitsudome et al. [11] reported high conversions and selectivities (80-95%) in the selective oxidation reactions of C_3-C_{18} olefins over Pd^{2+}-exchanged montmorillonite clay in N,N-dimethylacetamide solvent, containing $CuCl_2$ co-catalyst. Palladium salts of heteropolyacids of the Keggin-series ($H_{3+n}PV_nMo_{12-n}O_{40}$) supported on silica were successfully applied for selective oxidation of ethylene [12] and 1-butene [13]. However, in both systems the conversion and selectivity in the formation of carbonyl compounds showed fast decrease and the catalytic activity was rapidly lost. Vanadia, supported on various oxides (SiO_2 [14], Al_2O_3[15,16] and TiO_2 [17]) and doped with palladium showed good activity in vapour phase oxidation of alkenes. Studies showed that TiO_2 supported Pd/V_2O_5 redox system is more active in the Wacker oxidation of propylene to acetone [14] or 1-butene to butanone [17] than the corresponding SiO_2 or Al_2O_3 supported catalysts. Evnin et al. [15] ascertained that titanium acts on the V_2O_5 phase as a p-type dopant. As such, it should lower the Fermi level of the system and create a depletion layer near to the surface, thereby, increase the electron mobility and make the whole system

more “reducible”. Stobbe-Kreemers et al. [17] proved the higher reducibility of V_2O_5 on TiO_2 than on Al_2O_3 by means of X-ray photoelectron spectroscopy (XPS) and temperature-programmed reduction (TPR) measurements. The XPS spectra gave information about the steady-state surface concentration of Pd^{2+} and Pd^0 for catalysts used in Wacker oxidation of olefin. A significant amount of zero valent palladium was detected in the alumina-supported catalysts indicating that the re-oxidation of Pd^0 by the vanadium oxide layer under steady-state reaction conditions is slow. In contrast, no Pd^0 was observed over the titania-supported catalysts, suggesting that the re-oxidation of Pd^0 by the V_2O_5 was either fast on this support or there was hardly any formation of Pd^0.

Studies reveal that V_2O_5 supported on TiO_2 is more active in gas phase non-Wacker oxidation reactions by O_2 than the V_2O_5 on Al_2O_3 or SiO_2 support. Deo et al. [18] studied the partial oxidation of methanol to formaldehyde and observed that the turnover frequency (TOF) of the reaction was two order of magnitude higher over V_2O_5/TiO_2 than over V_2O_5/Al_2O_3 and three order of magnitude higher than over V_2O_5/SiO_2 catalyst. Similarly, the TiO_2 appeared to be the support of the most active supported V_2O_5 catalyst in the oxidation of formaldehyde to formic acid [19].

The outstanding activity of V_2O_5/TiO_2 catalysts was recently reviewed by Haber [20]. The formation of the surface vanadium oxide layer on the support before the formation of crystalline V_2O_5 phase is a consequence of the high surface mobility of vanadium oxide, which stem from lower surface free energy of crystalline V_2O_5 than that of the TiO_2 [21]. The migration of vanadium oxide was observed only over the surface of the anatase form titania. The reactivity (and reducibility) of V_2O_5/TiO_2 is supposed to be related to the V-O-Ti bond strength [18]. The spreading of vanadia over the surface of the support increases the number of V-O-Ti bonds and leads to more reducible and active catalyst.

When a solid catalyst is contacted with a liquid phase reaction mixture it is often questioned whether the activity could be associated with the effect of surface active site ensembles because leaching of metal particles can result in an active homogeneous catalyst [22]. Heterogeneous catalytic effect can be proved by filtration separation of the supported catalyst and testing activity in the filtrate. In vapour phase reactions catalyst leaching is less probable. However, the boiling point (vapour pressure) restricts the number of olefins which can be converted in gas phase.

The aims of present study are to gain better understanding of the catalytic effect of $Pd/V_2O_5/TiO_2$ catalysts in the Wacker-type oxidation of ethylene, the influence of palladium and vanadia loading and reactant partial pressures on the activity and selectivity of the catalysts. The consecutive oxidation of partially oxidized products, acetaldehyde and acetic acid, is also discussed.

2. Experimental

2.1 Catalyst preparation

The catalysts were prepared using solution, containing decavanadate ($V_{10}O_{56}^{6-}$) ions, formed from solution, containing metavanadate (VO_3^-) ions. Ten grams of ammonium metavanadate (NH_4VO_3, VEB Laborchemie, Apolda, 99.0 % purity) was dissolved in 1 dm^3 distilled water and, in order to obtain decavanadate ions, the pH of the solution was adjusted to pH=4 by addition of 0.1 mol/dm^3 HNO_3 solution. Calculated amounts of decavanadate solution was added to previously dried TiO_2 (Aeroxide TiO_2, P-25, Evonik Industries AG) to obtain 2.1, 4.2 and 8.4 wt% V_2O_5 in V_2O_5/TiO_2 preparations. In the next step the solvent water was evaporated, and the obtained solid was dried at 120 °C overnight, and calcined at 400 °C for 4 h. Using $Pd(NH_3)_4(NO_3)_2$ (5.0 wt% Pd as solution, Strem Chemicals Inc.) a solution was made containing 4 g/dm^3 Pd. Catalysts of about 0.01, 0.1, and 0.4 wt% Pd

content were obtained by impregnating the above described V_2O_5/TiO_2 preparations with calculated amount of the Pd solution. Preparations were dried and calcined at 400 °C for 4 h.

The vanadium contents of the preparations were expressed in V_2O_5 equivalents. The vanadia/titania samples are designated with a number giving the V_2O_5 content in weight percent and letter V, such as 2.2V, 4.6V and 8.6V. An example for the designation of the Pd-containing samples is 0.4Pd4.6V, where the number in front of the Pd symbol gives the Pd content in weight percent.

Characterization of catalysts

2.2.1. Specific surface area

Specific surface area (SSA) of the catalysts was obtained by the BET method from N_2 adsorption isotherm determined at -195°C by using Quantachrome NOVA Automated Gas Sorption Instrument. Before measuring adsorption isotherms samples were outgassed by vacuum at 150 °C for 24 h.

2.2.2. Elemental analysis

The palladium and vanadium content of catalysts was determined by means of Inductively Coupled Plasma Optical Emission Spectrometer (ICP-OES) equipped with polychromator, array detector, and applying axial viewing of the plasma (SPECTRO Analytical Instruments GmbH). For the measurements 100 mg of catalyst sample was rendered soluble by digesting it in 50 ml of boiling concentrated sulphuric acid for 2 hours. Individual calibration curve was recorded for each component in 50 vol% sulphuric acid solution in order to eliminate errors that could be caused by the use of common nitric acidic standards, having densities different from that of the sample solutions.

2.2.3. X-ray powder diffraction

X-ray patterns were recorded by Philips PW 1810/3710 diffractometer applying monochromatized Cu Kα radiation (40 kV, 35 mA). The patterns were recorded at ambient conditions between 3° and 65° 2Θ, in 0.02° steps, counting in each step for 0.5 s.

2.2.4. FT-Raman spectroscopy

Raman spectra were recorded with a dynamically aligned BIO-RAD Digilab Division dedicated FT-Raman spectrometer equipped with a Spectra-Physics Nd-YAG-laser (1064 nm) and high sensitivity liquid-N_2 cooled Ge detector. The laser power used was about 250 mW at the samples. The resolution of the Raman instrument was 4 cm^{-1}. A backscattered geometry was used. For each spectrum 256 individual spectra were averaged. The obtained spectra were normalized to the most intense band of the TiO_2 support at 145 cm^{-1}.

2.2.5. Temperature-programmed reduction by hydrogen (H_2-TPR)

A flow-through microreactor made of quartz tube (I.D. 4 mm) was used. About 100 mg of catalyst sample (particle size: 0.63–1.00 mm) was placed into the reactor and was treated before the measurement in a 30 cm^3 min^{-1} flow of O_2 at 350 °C for 1 h. Then the sample was cooled to room temperature in N_2 flow, flushed for 30 min and contacted then with a 30 cm^3 min^{-1} flow of 10% H_2/N_2 mixture. The reactor temperature was ramped up at a rate of 10 °C min^{-1} to 600 °C and kept at this temperature for 1 h while the effluent gas was passed through a trap, cooled by liquid nitrogen, and a thermal conductivity detector (TCD). Data were collected and processed by computer. The hydrogen consumption was calculated from the area under the H_2-TPR curve. The system was calibrated by determining the H_2-TPR curve of CuO reference material.

2.2.6. X-ray photoelectron spectroscopic(XPS) measurements

Spectra were measured using an electron spectrometer made by OMICRON Nanotechnology GmbH (Germany). The photoelectrons were excited by MgKα (1253.6 eV) radiation. Spectra were recorded in constant analyzer energy scan mode of EA125 Energy Analyser with 30 eV pass energy resulting in a spectral resolution of 1 eV.

Pellets, pressed from powdered samples, were fixed to standard OMICRON sample plates. Samples were either annealed in high vacuum or treated in the high-pressure chamber of the spectrometer in 300 mbar H_2 at elevated temperatures. Spectra of vanadium(V)oxide and vanadium (III)oxide were determined and used as reference to assign XPS peaks of the catalyst samples to vanadium species in different chemical states.

The non-reduced samples were charging heavily. A fortunate situation is that in both vanadium oxides [23] and TiO_2 [24-26] the leading contribution to the O 1s spectrum appears around 530.0 eV, thus a relatively reliable binding energy scale (containing no more uncertainity than 0.1-0.2 eV) can be obtained by setting the binding energy of the maximum of the O 1s envelope to this value. According to the literature, this calibration is much better than the one using the binding energy of the C 1s peak of hydrocarbon contamination as reference value [27].

Data were processed using the CasaXPS software package [28] by fitting the spectra with Gaussian-Lorentzian product peaks after removing a Shirley background. Nominal surface compositions were calculated using the XPS MultiQuant software package [29,30] with the assumption of homogeneous depth distribution for all components. XPS databases were used to identify the chemical states of vanadium [31,32].

2.2.7. Catalytic activity measurements

Catalytic test reactions were carried out at atmospheric pressure in a fixed-bed, continuous flow tubular microreactor. Prior to the reaction the catalysts were activated in oxygen flow (20 cm^3 min^{-1}) for 1 h at 350 °C. The same treatment was applied to re-activate used catalysts. In the catalytic test $C_2H_4/O_2/H_2O$/He gas mixture was fed on 500 mg of catalyst sample (particle size 0.63-1.00 mm). The partial pressures of ethylene, oxygen, and water were 3.4, 13.5, and 27 kPa, respectively. In oxidation tests of acetaldehyde and acetic

acid, the partial pressure of latter reactants was kept at 1.7 kPa, whereas the oxygen and water partial pressures were the same as during ethylene oxidation tests. The effect of the partial pressures on the activity was studied by varying the partial pressure of oxygen and water in the ranges of 6.4-52.2 and 0-56.4 kPa, respectively, on expense of the partial pressure of the helium carrier gas The space time of reactants ethylene, acetaldehyde, and acetic acid was either 205 h g_{cat}. $mol^{-1}_{reactant}$ or 410 h g_{cat} $mol^{-1}_{reactant}$, except when the space time dependence of ethylene or acetaldehyde conversion was studied. In the measurements of partial pressure and space time dependence 100 mg of catalyst, diluted with 400 mg of inert γ-Al_2O_3 was used. The total flow rate of the reaction mixture was always 30 cm^3 min^{-1}. All gas lines of the apparatus were heated to 120 °C in order to avoid condensation of water and reaction products. The reaction products were analysed by on-line Shimadzu GC-2010 gas chromatograph (GC) equipped with a 30-m HP-PLOT-U column, thermal conductivity and flame ionization detectors (TCD and FID). The calibration of the GC for each reactant and product compound was carried out separately. The conversion of ethylene was calculated from the ethylene concentrations in the feed and effluent. Selectivities were calculated from molar product composition.

3. Results and discussion

Specific surface area and contents of palladium and vanadia of fresh and used catalysts are given in Table 1. Deposition of V_2O_5 and Pd on TiO_2 resulted in catalysts, having only slightly smaller specific surface areas (SSA) than the pure titania support (SSA=55 m^2 g^{-1}). The catalytic activity and selectivity of the fresh catalysts could be reproduced using re-activated catalysts. Therefore, the effect of reaction conditions on the activity could be studied over a single catalyst charge that was always re-activated before reaction conditions were changed. Neither the activity nor the selectivity changed in 20 h time-on-stream. After several

days in contact with the reacting mixture under varying conditions the chemical composition of the catalysts was determined again. Results suggest that no significant compositional change occurred (Table 1).

The catalytic activity strongly depends on the dispersion and structure of the supported vanadium-containing species. Monolayer surface coverage corresponds to approximately 7 to 8 VO_x species on a square nanometer of titania surface [33]. In case of titania P-25 the monolayer coverage amounts to about 6 wt% V_2O_5 content. The V_2O_5 content of our catalyst preparations was either far below the monolayer coverage (2.2 wt%) or strongly exceeded it (8.6 wt%). One of our catalysts contained 4.6 wt% V_2O_5, i. e., the V_2O_5 loading of the titania support was near to that corresponding to monolayer coverage (Table 1). The XRD patterns in Fig. 1 show that crystalline V_2O_5 was present in the sample of highest vanadia content only. Reflections of anatase and rutile appear in the XRD pattern of each sample.

The Raman spectra of titania-supported V_2O_5 samples are presented in Fig. 2. In the wavenumber region below 800 cm^{-1} only the intense absorption bands of TiO_2 support (~ 145, 397, 515 and 638 cm^{-1}) are present (not shown). Between 800 and 1200 cm^{-1}, except for the catalyst with the lowest vanadia coverage, a single band appeared at 995 cm^{-1}. This band can be assigned to crystalline V_2O_5 particles. The strength of the band increases with increasing vanadia loading. The V_2O_5 reflections and Raman band are somewhat stronger for the 8.6V sample prepared by mechanically mixing V_2O_5 and TiO_2 than those of the chemically prepared 8.6V preparation, indicating that vanadia is present in slightly different forms in the two samples. The finding that the Raman band of crystalline V_2O_5 at 995 cm^{-1} appears also in the spectrum of 4.2 wt% V_2O_5/TiO_2 catalyst can be explained by the much larger Raman scattering cross section of crystalline V_2O_5 than that of dispersed monovanadate and polyvanadate structures [34]. Traces of crystalline V_2O_5 gave Raman band but could not generate X-ray reflection signals.

H_2-TPR measurements were carried out to characterize the reducibility of catalysts. The TPR profiles of V_2O_5/TiO_2 and $Pd/V_2O_5/TiO_2$ samples are shown on Fig. 3. In absence of palladium the reduction of V_2O_5 phase proceeds between 300 and 600°C for each sample. The change in the oxidation state of the vanadium atoms upon reduction was determined by integration of the H_2-TPR peaks. As Table 2 shows that the H_2/V values obtained for the V_2O_5/TiO_2 samples varies between 1.13 and 1.27, corresponding roughly to the reduction of V^{5+} to V^{3+}. On the profiles of palladium containing samples two reduction peaks are present: a sharp low-temperature peak below 200°C and a broad high-temperature peak overarching the whole temperature range of the measurement. The reduction of palladium, supported on TiO_2 takes place around 0°C [35]. Thus, the formation of metallic palladium occurs immediately when the N_2 flow is switched to H_2/N_2 flow. The Pd/TiO_2 (not shown) and 0.4Pd2.1V samples present negative peaks in region 50-180 °C, which are assigned to release of hydrogen absorbed in Pd^0 crystallites at lower temperature. At low vanadia loadings the released hydrogen could mask hydrogen consumption but at higher loadings no negative H_2 desorption peaks could be discerned. Van der Heide [36] showed that the low-temperature reduction of V_2O_5 proceeds via a hydrogen spill-over process in which hydrogen is dissociatively chemisorbed at the palladium surface and chemisorbed hydrogen atoms move form palladium to the surrounding vanadium oxide. The spill-over experiments showed no formation of water at 373 K, only the uptake of hydrogen. Moreover, hardly any weight change was observed during hydrogen uptake. They concluded that the V_2O_5 monolayer is transferred into a monolayer of a hydrogen bronze of vanadium ($H_xV_2O_5$ x=1.4 to 2) and not into lower valence vanadium-oxides. In our experiments H_2/V values between 0.49 and 0.66 were obtained for palladium containing samples (Table 2) that suggests only one-electron reduction ($V^{5+} \rightarrow V^{4+}$). Latter result is in conflict with our earlier findings with different oxide-

supported Pd/vanadia catalysts, where always near to two-electron reduction was attained in similar H_2-TPR measurements [37, 38].

In order to find explanation for the unexpected one-electron reduction we accomplished a detailed XPS study on the 8.6V and 0.4Pd8.6V catalysts. V_2O_5 and V_2O_3 were used as reference materials (Figure 4A). The XPS spectrum of the reference materials was recorded first in their "as received" state, i.e., without applying any thermal or reductive treatment. For both samples V^{5+} was found to be the dominant surface vanadium species. The V 2p spectrum of V_2O_5 is dominated by the narrow $2p_{3/2}$ line of V^{5+} at 517.1 eV, separated from the main O 1s contribution by 12.8-12.9 eV. These data are in good agreement with the XPS characteristics of these compounds published earlier [39]. In addition to the main V $2p_{3/2}$ peak, a small contribution is also present at about 515.5 eV. It is assigned to the photoelectron peak of V^{4+} ions, the presence of which is interpreted as a result of photoinduced V_2O_5 reduction (Figure 4A, lowermost spectrum).

The V_2O_3 reference sample was studied also after 2 hours of vacuum annealing at 230°C. The treatment transformed the surface layer of the "as received" sample into a mixed valence V_6O_{13} –like compound as suggested by the shape of the valence band spectrum [40]. The spectrum of the O 1s and V 2p region of the sample is shown in Figure 4A (uppermost spectrum). Instead of the narrow V $2p_{3/2}$ line, seen in the spectrum of V_2O_5, a broad band appeared shifted towards lower binding energies. This band was deconvoluted into a narrow band at 517.1 eV and another rather broad feature centered at 516.1 eV. The narrow and the broad bands were shifted from the main O 1s contribution by 12.8 eV (V^{5+}) and 14.0 eV, respectively. Latter can be identified as contribution from V^{4+} ions [39]. Presence of e V^{4+} ions is confirmed also by the appearance of a weak peak in the valence band region, above the O 2p-related edge, in the vicinity of the Fermi level, which arises from filled V 3d states.

The V 2p region of the 8.6V sample in the “as received” state shows a narrow V $2p_{3/2}$ component at a binding energy of 517.1 eV, what indicates that the most abundant vanadium species in this sample is V^{5+}. Nevertheless, the low binding energy component at 516.0 eV (V^{4+}) is clearly stronger than that in the spectrum of the V_2O_5 reference sample (Figure 4A). It is to be noticed that the sample is somewhat unstable against X-ray exposure, as this V^{4+} component clearly increases during the measurement. In order to minimize this effect, in all experiments the V 2p region was recorded prior to any other spectral region. Titanium was found to be in its fully oxidized state (Ti^{4+}). The Ti $2p_{3/2}$ binding energy corresponds to literature values. No reduction of titanium was observed during the measurements.

Figure 4A also shows the XPS spectra of 8.6V V_2O_5/TiO_2 sample, obtained after H_2 treatment at different temperatures. Spectra were recorded without exposing the sample to air after the treatments. Treatment at 100°C left the majority of vanadium in V^{5+} state. The V^{4+} contribution was not enhanced by the treatment. Composition was calculated from the XPS data. The vanadium content was expressed in V_2O_5 and is given in weight percents. Accordingly, the surface layer, available for XPS analyses, contains 19 wt% V_2O_5, indicating that vanadia covers large fraction of the titania surface and prevents it from being detected by XPS.

The treatment at 200 °C did not affect the chemical state of Ti^{4+} but a clear increase was noticed in the intensity of the V^{4+} component of the V $2p_{3/2}$ band.

The H_2 treatment at 300°C caused significant changes relative to the previously recorded XPS spectrum of the 8.6V sample. The V $2p_{3/2}$ band became broad and without structure. No sharp V^{5+} contribution could be identified by either simple inspection or curve fitting. The band center shifted obviously to binding energy that is lower than the 516.0 eV binding energy of V^{4+}. According to the literature, the broad V $2p_{3/2}$ band of V^{3+} appears

roughly around a binding energy of 515.2 eV [39]. Most probably vanadia, containing mixture of V^{4+} and V^{3+} ions, is present on the titania surface after the applied treatment.

The lowering oxidation state of vanadium was paralleled by the decreasing amount of XPS detectable vanadium. The obtained 13 wt% V_2O_5 content indicated that the surface layer was depleted from vanadium. It may be either due to diffusion of vanadium ions into deeper layers of the TiO_2, due to decrease of dispersion of the vanadium-oxide or due to evaporative loss, if volatile oxide- or hydroxide-like vanadium compound was formed. It is to be noted that no vanadium loss was detected during catalytic tests, which were carried out at temperatures below 200 ^{o}C (Table 1).

Upon reduction at 400°C the rather weak but still broad V $2p_{3/2}$ peak shifted to 515.2 eV, which corresponds to the binding energy reported for V_2O_3. The detected 6 wt% V_2O_3 content shows that the treatment enhanced the depletion of vanadium from the surface of the 8.6V sample.

Fig. 4B shows XPS spectra of the Pd-containing V_2O_5/TiO_2 catalyst 0.4Pd8.6V. The V 2p region of the "as received" sample contains a narrow V $2p_{3/2}$ component at binding energy 517.1 eV, along with a much broader peak around 516.2 eV, indicating that the V^{4+} contribution is already significant. The sample was strongly unstable against X-ray exposure, as this V^{4+} component rapidly increased and became dominant during the measurement. The bulk vanadium content of the 0.4Pd8.6V sample was essentially the same as that of the corresponding Pd-free sample, whereas that of the surface layer was equivalent with a concentration of 18 wt% V_2O_5. Titanium maintained its fully oxidized state during the measurements, i.e., the Ti $2p_{3/2}$ peak appeared and remained at the binding energy published for Ti^{4+} in the literature.

The 1h reduction at 100°C resulted in no significant change in the surface composition. The vanadium chemical states were, however, notably influenced. The V $2p_{3/2}$

region shows a broad and asymmetric envelope which can be deconvoluted into a V^{5+} component at 517.1 eV and a broad peak at 516.1 eV, which can be attributed to V^{4+} ions (Fig. 4B).

The hydrogen treatment at 200°C resulted in a further reduction of vanadia. The peak shape of the broad V $2p_{3/2}$ feature and the corresponding binding energy resemble now to those of the Pd-free sample reduced at 300°C. The surface vanadium concentration, expressed in V_2O_5, decreased to 15% (Fig. 4B).

The reduction at 300°C did not brought about noticeable change in the surface composition (Fig. 4B). The broad V $2p_{3/2}$ peak around 515.4 eV indicated that the vanadium was mostly in V^{3+} ionic state. Reduction of TiO_2 was still not detectable.

The reduction at 400°C resulted in a minor shift of the broad V $2p_{3/2}$ peak to 515.3 eV and decreased the surface V_2O_5 concentration to 12 wt% (Fig. 4B).

The relative amounts of vanadium in high (V^{5+}) and lower oxidation states (V^{4+}, V^{3+}) determined from the spectra of Fig. 4, are visualized in Fig. 5. The 8.6V sample is significantly more resistant to reduction than the 0.4Pd8.6V sample. At temperature whereon the V^{5+} ions of the Pd-free sample only began to get reduced, all the V^{5+} ions of the Pd-containing sample became reduced to V^{4+} and V^{3+}.

For the above characterized samples X-ray induced Auger spectra of vanadium are shown in Fig. 6. As the vanadium $L_{23}M_{23}M_{45}$ Auger transition involves electrons from the valence band, the obtained line shape is very sensitive for the electron population of the 3d orbitals that is increasing as the oxide undergoes reduction. For V_2O_5 a relatively symmetric line was found at kinetic energy 466.2 eV. Sambi et al. [25] reported that reduction of supported vanadia shifts the maximum of the Auger line towards higher energies giving rise to a new component at 472-473 eV, which is indicating the appearance of filled vanadium 3d orbitals. Our results are in accordance with these findings. The kinetic energy and shape of the

$L_{23}M_{23}M_{45}$ Auger line suggests that V^{5+} is the major vanadium species of the 0.4Pd8.6V sample in the "as received" state, although the V^{4+} contribution is already significant. Upon H_2 treatment at 100°C no significant changes occurred. After reduction at 200°C the V $L_{23}M_{23}M_{45}$ Auger band appeared with center around 469 eV together with a very significant contribution around 472 eV. The line shape starts to resemble the two-peaked feature reported for V_2O_3 what indicates that the sample at this point contains a mixture of V^{4+} and V^{3+} ions, with the probable dominance of the latter species. The spectrum recorded after reduction at 300°C corresponds to the shape of that reported for V_2O_3 suggesting that V^{3+} is the prevailing vanadium species. On effect of reduction at 400°C the Auger line broadens towards the low kinetic energy side. Similar spectrum was obtained for sample 8.6V, reduced at or above 300°C (Fig. 6).

Results of XPS measurements suggest that the average H_2/V values close to 0.5 are not due to the one electron reduction of V^{5+} to V^{4+}. The oxidation state of vanadium in the deeply reduced palladium doped samples was found to be V^{3+}. Results substantiate that vanadium already was not in its fully oxidized V^{5+} state when recording of the H_2 consumption in the H_2-TPR measurements was started. This can explain that lower amount of H_2 was consumed to reach the final V^{3+} state than was needed starting the reduction from V^{5+} state.

The Wacker oxidation of ethylene was studied over $Pd/V_2O_5/TiO_2$ catalysts, having different Pd loadings. When the Pd loading of the 2.1V support was raised from 0.01 to 0.1 wt% the conversion of ethylene significantly increased (Fig. 7). As a result higher acetaldehyde yield was obtained even at decreasing acetaldehyde selectivity. Much higher Pd contents hardly affected product distribution. The selectivity of CO_2 slightly increased on expense of the selectivity of partially oxidized products. Based on these results V_2O_5/TiO_2 catalysts of 0.4 wt% Pd content were chosen for detailed catalytic examination.

Fig. 8 shows the effect of oxygen and water partial pressure on the conversion and selectivity of ethylene oxidation over 0.4Pd4.6V catalyst at 125 °C. At low oxygen partial pressures (< 15 kPa) the conversion and selectivity of products is almost constant. At higher oxygen partial pressures both the ethylene conversion and the acetic acid and CO_2 selectivity are higher but the acetaldehyde selectivity is lower (Fig. 4A). These results are in accordance with the picture of a consecutive oxidation process where acetaldehyde is the primary product that becomes further oxidized to acetic acid or CO_2. Dependence of ethylene conversion and product selectivity on the partial pressure of water is shown in Fig. 8B. In absence of water in system ethylene becomes converted to CO_2 only. At higher water partial pressure higher acetaldehyde selectivity is obtained at relatively low ethylene conversion. Above about 40 kPa water partial pressure the selectivities are virtually independent from the water content of the reaction mixture. Only slight increase of ethylene conversion was observed, whereas the CO_2 selectivity dropped to about 5%.

The effect of space time on conversion of ethylene and acetaldehyde and on the yield of the main products was examined using 0.4Pd4.2V catalyst at 150 °C (Fig. 9). The yield of acetaldehyde (Fig. 9A) passes through maximum indicating that this product is intermediate of a consecutive oxidation process. In the Wacker conversion of acetaldehyde crotonaldehyde has a concentration maximum at low space times, indicating that aldol condensation of acetaldehyde takes place. No concentration maxima were observed for acetic acid suggesting that it is not intermediate to CO_2 formation (Fig. 9B).

Results of ethylene Wacker oxidation over $Pd/V_2O_5/TiO_2$ catalysts with different vanadia contents are shown as function or reaction temperature in Fig. 10. The main reaction products are acetaldehyde, acetic acid and CO_2. The formation of methane and acetone was also detected but in negligible amounts. At low temperatures (100-125°C) acetaldehyde is the main product irrespectively of vanadia content. At higher temperatures the selectivities of

acetic acid and CO_2 rapidly increases and at 200°C the oxidation to CO_2 becomes the main reaction. Between 125 and 175°C the formation of acetic acid and CO_2 is almost equimolecular. The catalysts of higher vanadia content show similar ethylene conversion activity (Fig. 10A). The highest acetaldehyde yields were obtained with the catalyst having close to monolayer vanadia coverage on the titania support (~65 % at 100 °C, see Fig. 10B). For Wacker activity the intimate contact of Pd and the VO_x particles is essential. The structure of surface vanadia has also importance. Fig. 10C demonstrates that a fraction of the primarily formed acetaldehyde becomes converted to acetic acid and CO_2 over Pd/vanadia redox pair at low temperatures. Low vanadia content corresponding to sub-monolayer coverage of titania support (Fig. 10A) results in lower ethylene conversion and higher acetaldehyde selectivity, whereas higher vanadia content, corresponding to about monolayer coverage results in higher ethylene conversion and lower acetaldehyde selectivity. The product distribution at 175-200 °C is almost the same for all catalysts.

Results of Wacker oxidation of ethylene is shown in Fig. 11A as function of reaction temperature over 0.4Pd4.6V in comparison with the conversion of the partially oxidized products, such as acetaldehyde (Fig. 11B) and acetic acid (Fig. 11C) over the very same catalyst under identical conditions. At low temperatures (100-125 °C) the conversion of acetaldehyde is low. At higher temperatures (≥150 °C) the acetaldehyde is converted to acetic acid and CO_2 in molar ratio close to 1 to 1. Formation of methane can be also observed with 5 to 10 % selectivity. Forni et. al. [41] substantiated that CO_2 formation takes place not only from acetaldehyde and acetic acid but, at least in part, directly from ethylene. Based on the results, shown on Fig. 11, direct oxidation of ethylene to CO_2 cannot be excluded, however, it is obvious that oxidation of acetic acid starts only above about 175 °C (Fig. 11C).

4. Conclusions

$Pd/V_2O_5/TiO_2$ catalysts gave high acetaldehyde yield in the selective oxidation of ethylene in presence of water at 100 °C. The highest acetaldehyde selectivity was achieved over catalyst with vanadia content corresponding to sub-monolayer coverage of the titania support. The conversion was low because of the small number of active Pd/VO_x redox couples. At high vanadia content V_2O_5 crystallites were formed on the surface of the support. Palladium on V_2O_5 crystallites has high oxidation activity and it converts the primarily formed acetaldehyde to acetic acid and CO_2 even at temperature as low as 100 °C. Regarding the acetaldehyde yield the favorable vanadia content is about equivalent with the amount needed to attain monolayer V_2O_5 coverage of the titania support. The results suggest that acetic acid and CO_2 are products obtained from primarily formed acetaldehyde. Oxidation of acetic acid to CO_2 occurs only above 175 °C.

Acknowledgement

This work was financially supported by the Hungarian Scientific Research Fund (OTKA, contract no. K 100411)

References

[1] J. Smidt, W. Hafner, R. Jira, J. Sedlmeier, R. Sieber, R. Rüttinger, H. Kojer, Angew. Chem. 71 (1959) 176-182.

[2] J. Smidt, W. Hafner, R. Jira, R. Sieber, J. Sedlmeier, A. Sabel, Angew. Chem. Int. Ed. 1 (1962) 80-88.

[3] A.S. Jhaveri, M.M. Sharma, Chem. Eng. Sci. 22 (1967) 1-6.

[4] R. Jira, in: B. Cornils and W.A. Herrmann (Eds.), Oxidation of Olefins to Carbonyl Compounds, Viley-VCH Verlag GmbH, Weinheim, 2002, pp. 386-405.

[5] R.A. Fernandes, D.A. Chaudhari, J. Org. Chem. 79 (2014) 5787−5793.

[6] S.F. Davison, B.E. Mann, P.M. Maitlis, J. Chem. Soc. Dalton Trans. 6 (1984) 1223-1228.

[7] P. Teo, Z.K.Wickens, G. Dong, R.H. Grubbs, Org.Lett. 14 (2012) 3237-3239.

[8] G. Centi, F. Cavani, F. Trifirò, Selective Oxidation by Heterogeneous Catalysis, first ed., Springer Science+Business Media New York, 2001.

[9] P.H. Espeel, M.C.Tielen, P.A.Jacobs, J.Chem. Soc. Chem.Commun.10 (1991) 669–671.

[10] E.D. Park, J.S. Lee, J. Catal. 180 (1998) 123–131.

[11] T. Mitsudome, T. Umetani, K. Mori, T. Mizugaki, K. Ebitani, K. Kaneda, Tetrahedron Lett. 47 (2006) 1425-1428.

[12] K. Nowińska, D. Dudko, Appl. Cat. A. 159 (1997) 75-87.

[13] A.W. Stobbe-Kreemers, G. van der Lans, M. Makkee, J.J.F. Scholten, J. Catal. 154 (1995) 187-193.

[14] M. Li, J. Shen, React. Kinet. Catal. Lett. 72 (2001) 263-267

[15] B. Evnin, J.A. Rabo, P.H. Kasai, J. Catal. 30 (1973) 109–117.

[16]A.W. Stobbe-Kreemers, M. Soede, M. Makkee, J.J.F. Scholten, Appl. Catal. A 131 (1995) 367–381.

[17] A.W. Stobbe-Kreemers, M. Makkee, J.J.F. Scholten, Appl. Catal. A 156 (1997) 219–238.

[18] G. Deo, I.E. Wachs, J. Catal. 146 (1994) 323-334.

[19] E.V. Danilevich, G.Ya. Popova, T.V. Andrushkevich, V.V. Kaichev, I.G. Danilova, Yu.A. Chesalov, V.A. Rogov, V.I. Bukhtiyarov, V.N. Parmon, Appl. Catal. A 475 (2014) 98–108.

[20] J. Haber, Catal. Today, 142 (2009) 100-113.

[21] I.E. Wachs, Dalton T. 42 (2013) 11762-11769.

[22] R.A. Sheldon, M. Wallau, I.W.C.E. Arends, U. Schuchardt, Acc. Chem. Res. 31 (1998) 485-493.

[23] J. Mendialdua, R. Casanova, Y. Barbaux, J. Electron Spectr. Rel. Phenom. 71 (1995) 249-261.

[24] Q. Guo, S. Lee, D.W. Goodman, Surf. Sci. 437 (1999) 38-48.

[25] M. Sambi, M. Della, Negra, G. Granozzi, Surf. Sci. 470 (2000) L116-L122,

[26] J. Biener, M. Bäumer, R.J. Madix, Surf. Sci. 432 (1999) 178-188.

[27] J. Mendialdua, R. Casanova, Y. Barbaux, J. Electron Spectr. Rel. Phenom. 71 (1995) 249-261.

[28] N. Fairley (2006). http://www.casaxps.com/.

[29] M. Mohai, Surf. Interface Anal. 36 (2004) 828–832.

[30] M. Mohai (2003). XPS MultiQuant: Multi-model X-ray photoelectron spectroscopy quantification program, Version 3.00.16
http://www.chemres.hu/aki/XMQpages/XMQhome.htm.

[31] C.D. Wagner, A.V. Naumkin, A. Kraut-Vass, J.W. Allison, C.J. Powell, J.R. Rumble Jr., NIST X-ray Photoelectron Spectroscopy Database, Version 3.4, National Institute of Standards and Technology, Gaithersburg, MD (2003) http://srdata.nist.gov/xps/,

[32] J.F. Moulder, W.F. Stickle, P.E. Sobol, K.D. Bomben: Handbook of X-ray Photoelectron Spectroscopy, Perkin-Elmer Corp. Eden Prairie, Minnesota, USA, 1992

[33] I.E. Wachs, B. M. Weckhuysen, Appl. Catal. A 157 (1997) 67–90.

[34] S. Xie, E. Iglesia, A. T. Bell, J. Phys. Chem. B 105 (2001) 5144-5152.

[35[C. Zhang, Y. Li, Y. Wang, H. He, Environ. Sci. Technol. 48 (2014) 5816-5822.

[36] E. van der Heide, M. Zwinkels, A. Gerritsen, J. Scholten, Appl. Catal. A 86 (1992) 181–198.

[37] R. Barthos, A, Hegyessy, Z, May, J. Valyon, Catal. Lett. 144 (2014) 702-710.

[38] R. Barthos, A, Hegyessy, Sz. Klébert, J. Valyon, Micropor. Mesopor. Mater. 207 (2015) 1-8.
[39] G. Silversmit, D. Depla, H. Poelman, G. B. Marin, R. De Gryse, J. Electron Spectr. Rel. Phenom. (2004) 135, 167-175.
[40] M. Demeter, M. Neumann, W. Reichelt, Surf. Sci. 454-456 (2000) 41-44
[41] L. Forni, G. Terzoni, Ind. Eng. Chem. Process. Des. Dev. 16 (1977) 288-293.

Figure legends

Fig. 1 XRD patterns of V_2O_5/TiO_2 preparations with different vanadia loadings. The diffractograms of the TiO_2 support (P25) and its mechanical mixture with 8.6 wt% V_2O_5 are given for comparison.

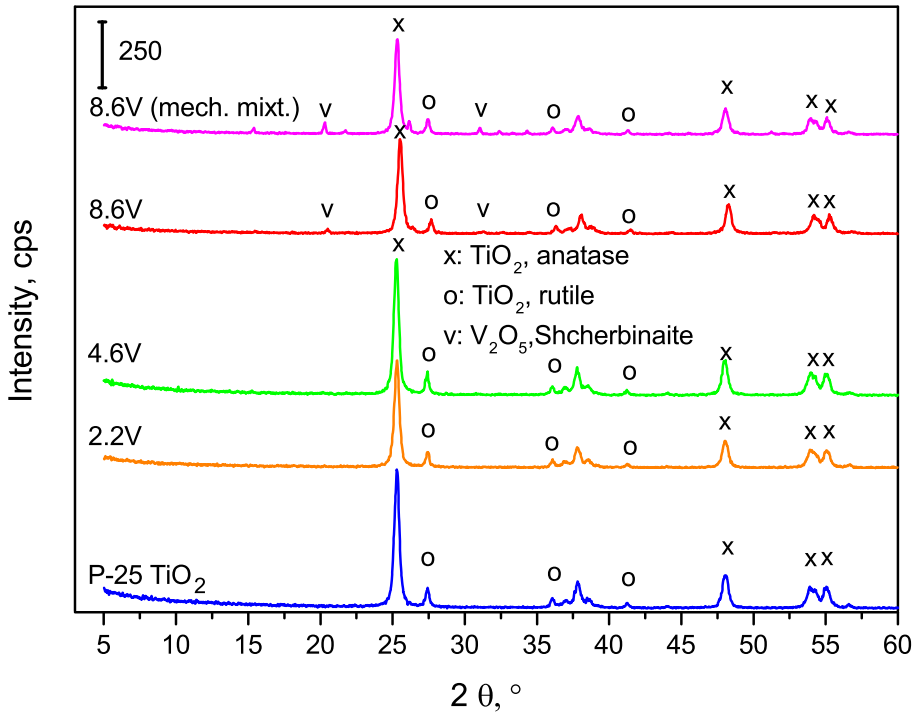

Fig. 1

Fig. 2, FT-Raman spectra of V_2O_5/TiO_2 preparations with different vanadia loadings. The spectra of the mechanical mixture of TiO_2 and 8.6 wt% V_2O_5 is given for comparison.

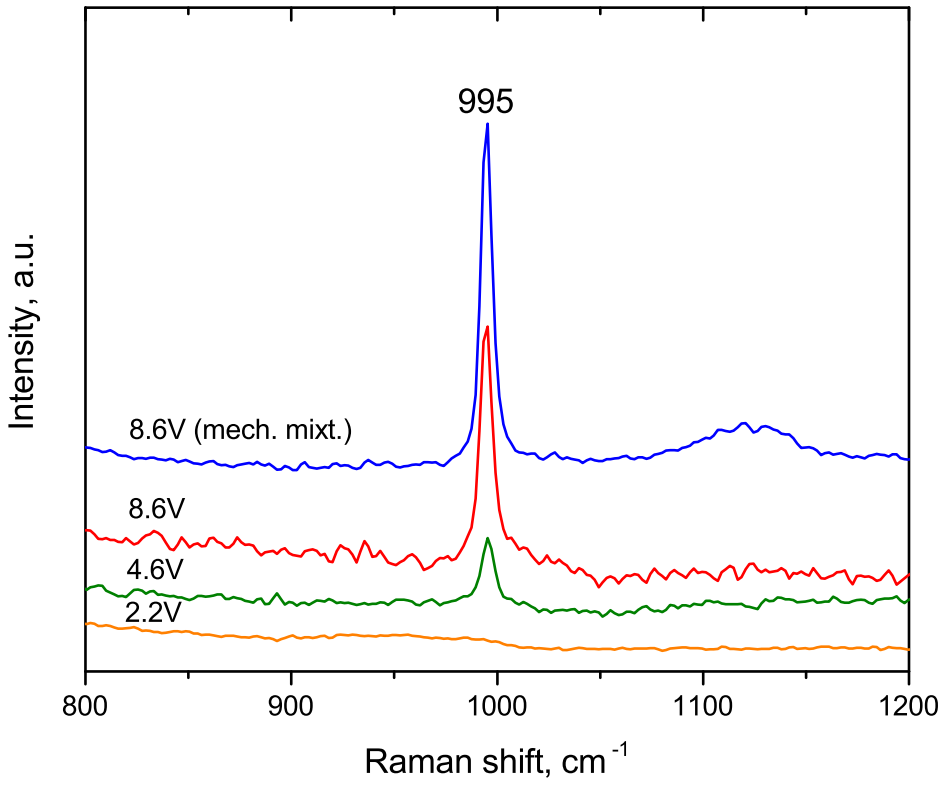

Fig. 2

Fig. 3. H_2-TPR profiles of V_2O_5/TiO_2 (dashed lines) and $Pd/V_2O_5/TiO_2$ (full lines) catalysts.

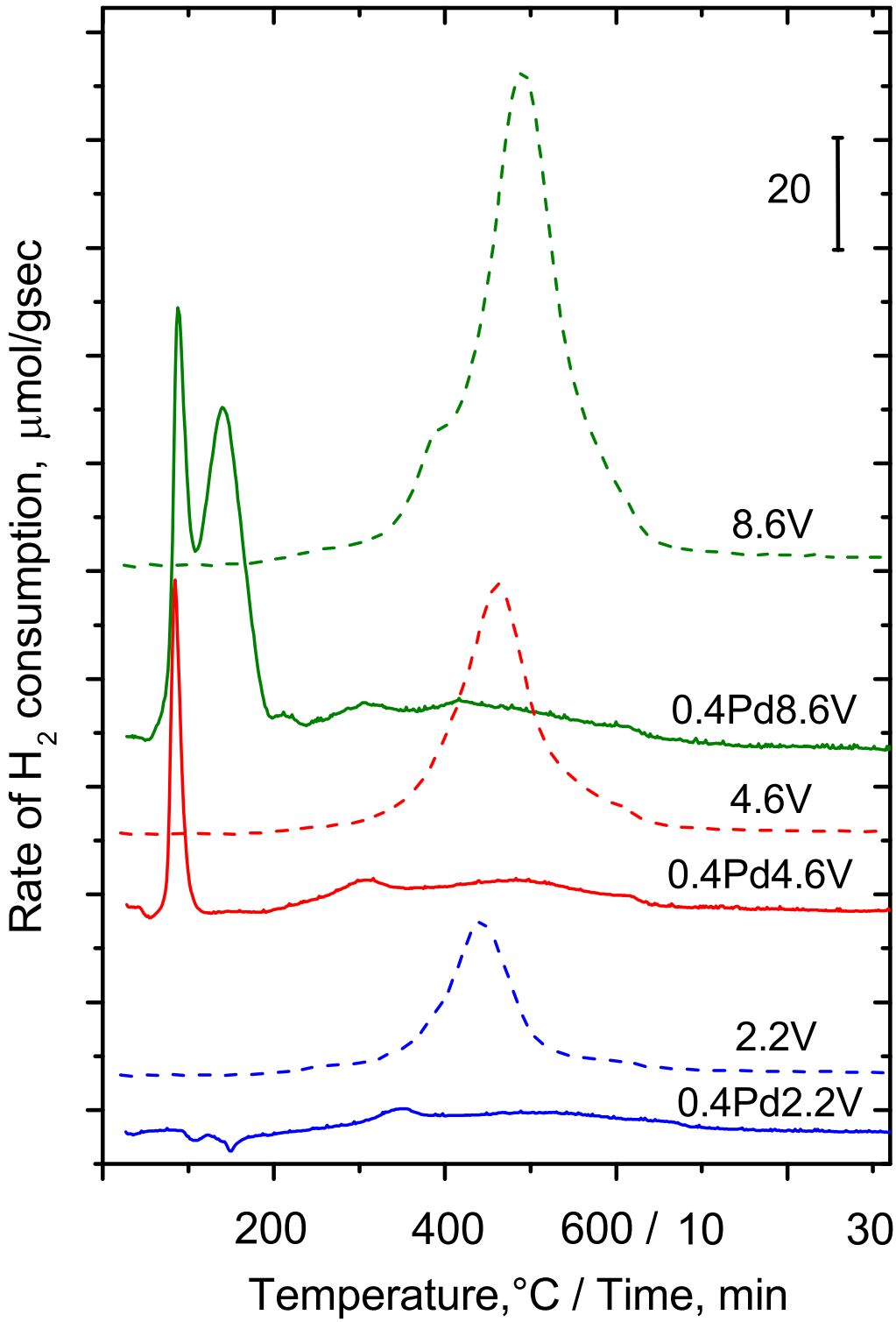
Rate of H2 consumption, µmol/gsec
20
8.6V
0.4Pd8.6V
4.6V
0.4Pd4.6V
2.2V
0.4Pd2.2V
200
400
600 / 10
30
Temperature,°C / Time, min

Fig. 3

Fig. 4. X-ray photoelectron spectra of the (A) 8.6V and (B) 0.4Pd8.6V samples in their untreated (as received) and treated states. Treatment involved heating the samples in 300 mbar H_2 successively at 100, 200, 300 and 400 °C for 1h at each temperature. Spectra are labelled by the treatment temperature only. The spectra were corrected for the $MgK\alpha_{3,4}$ contribution. In panel (A) also spectra of V_2O_5 and a V_6O_{13}-like compounds are shown for reference. Latter compound was obtained by vacuum annealing V_2O_3 at 230 ^oC. The reference spectra include both V 2p and O 1s contributions.

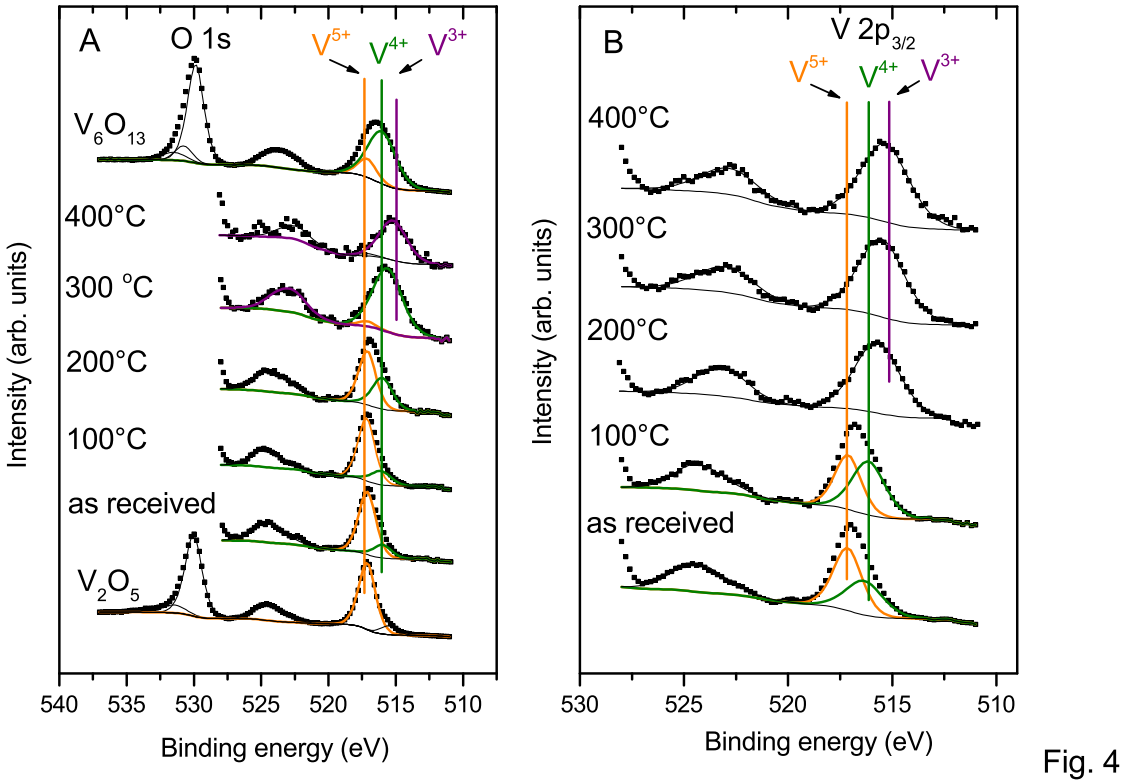

Fig. 4

Fig. 5. Relative amounts of vanadium in V^{5+} and lower oxidation states as function of the reduction temperature for the 8.6V and 0.4Pd8.6V samples. Data were derived from the spectra of Fig. 4.

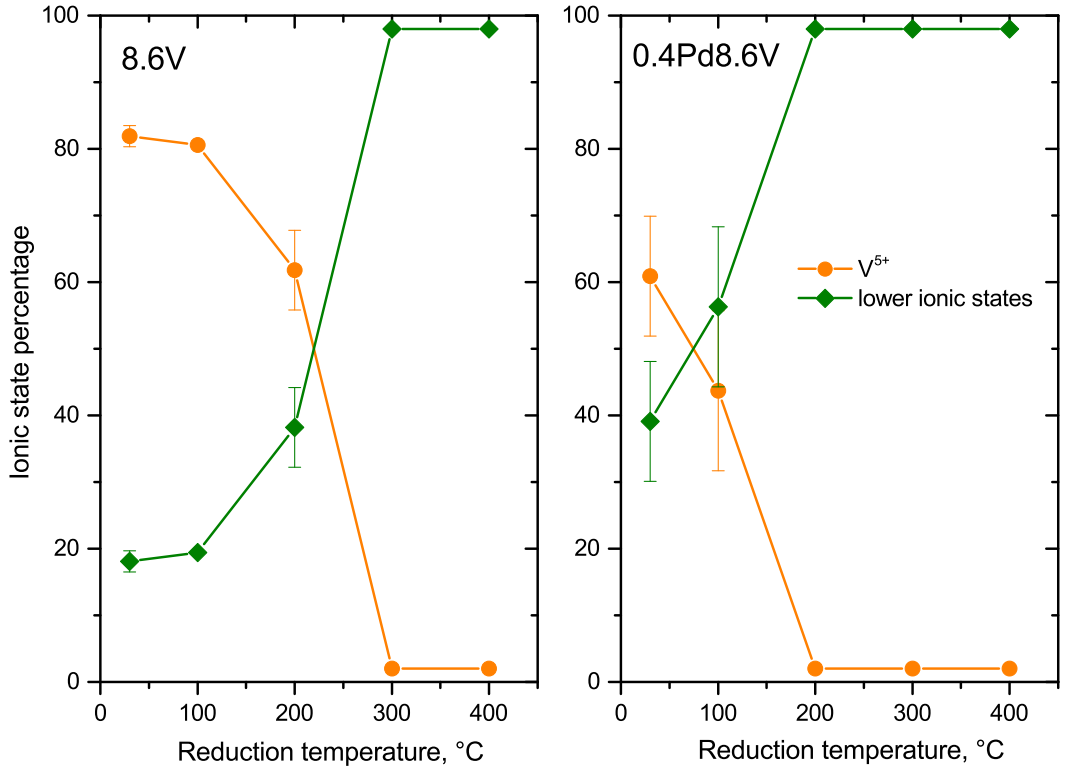

Fig. 5

Fig. 6. X-ray induced vanadium $L_{23}M_{23}M_{45}$ transition Auger spectra of samples 0.4Pd8.6V, 8.6V, and reference samples V_2O_5, and V_6O_{13} compounds. Spectra were obtained in the experiments described in the legend of Fig. 4. Spectra of sample 0.4Pd8.6V are labelled by the treatment temperature only.

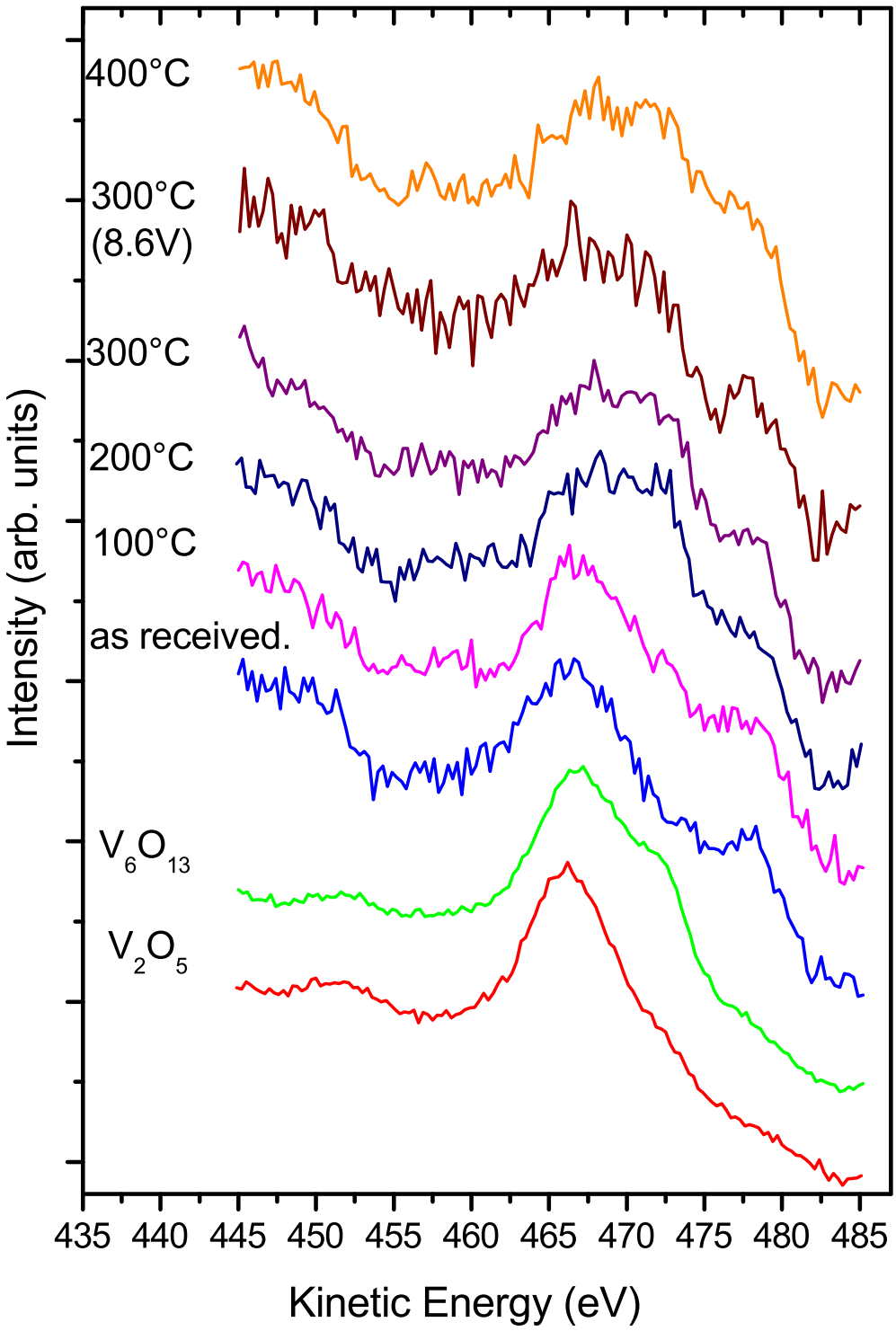
400°C
300°C
(8.6V)
300°C
200°C
100°C
as received.
V6O13
V2O5
Intensity (arb. units)
435 440 445 450 455 460 465 470 475 480 485
Kinetic Energy (eV)

Fig. 6

Fig. 7. The activity of $Pd/V_2O_5/TiO_2$ catalysts as a function of Pd content in the Wacker oxidation of ethylene at 150 °C. The 2.1V preparation was used to make Pd2.1V catalysts of different Pd contents. The space time was 205 h g_{cat}. $mol^{-1}_{ethylene}$. The partial pressures of ethylene, oxygen, and water in the $C_2H_4/O_2/H_2O$/He gas mixture were 3.4, 13.5, and 27 kPa, respectively.

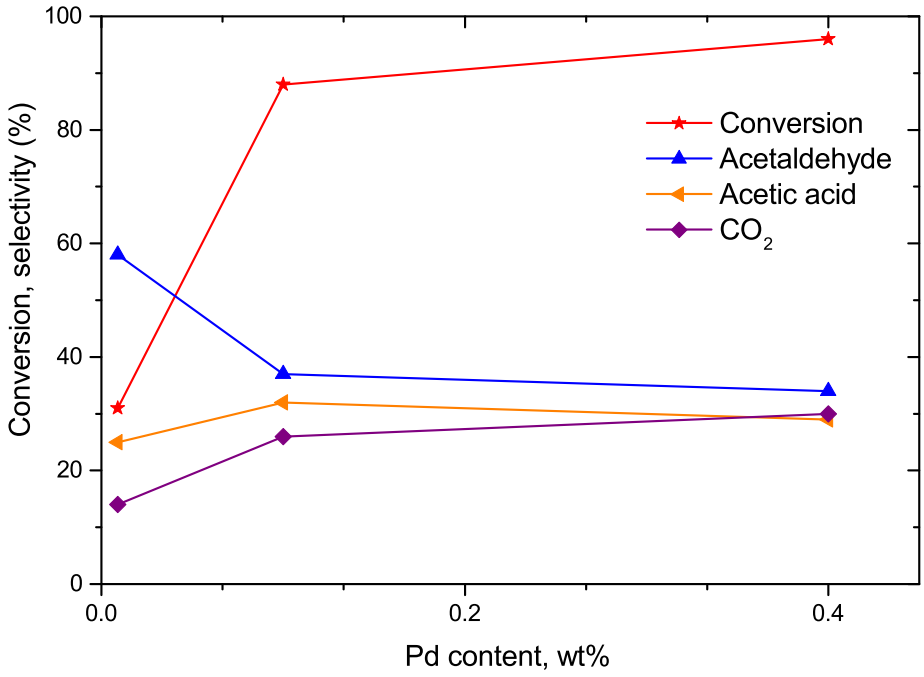

Fig. 7

Fig. 8. Effect of partial pressure of (A) oxygen and (B) water on the selective oxidation of ethylene at 125°C over 0.4Pd4.6V catalyst. 100 mg of catalyst was diluted by 400 mg of inert γ-Al_2O_3 to get a catalyst bed. The space time of ethylene was kept constant at 41 h g_{cat}. $mol^{-1}_{ethylene}$. The partial pressure of oxygen or water was changed on expense of the partial pressure of the He carrier gas.

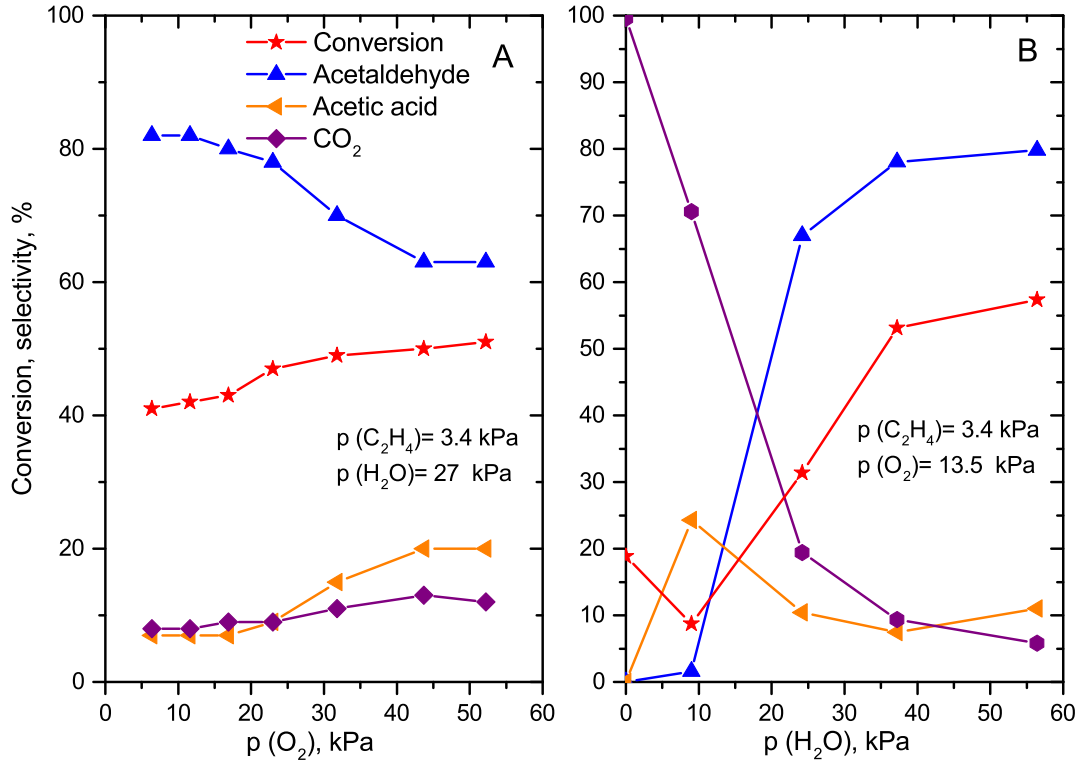

Fig. 8

Fig. 9. The Wacker oxidation of (A) ethylene and (B) acetaldehyde with O_2 in presence of water at varied reactant space time over 0.4Pd4.6V at 150 °C. 100 mg of catalyst was diluted by 400 mg of inert γ-Al_2O_3 to get a catalyst bed. The partial pressure of reactant acetaldehyde was kept at 1.7 kPa, The partial pressures of ethylene, oxygen and water were the same as those given in the legend of Fig. 7.

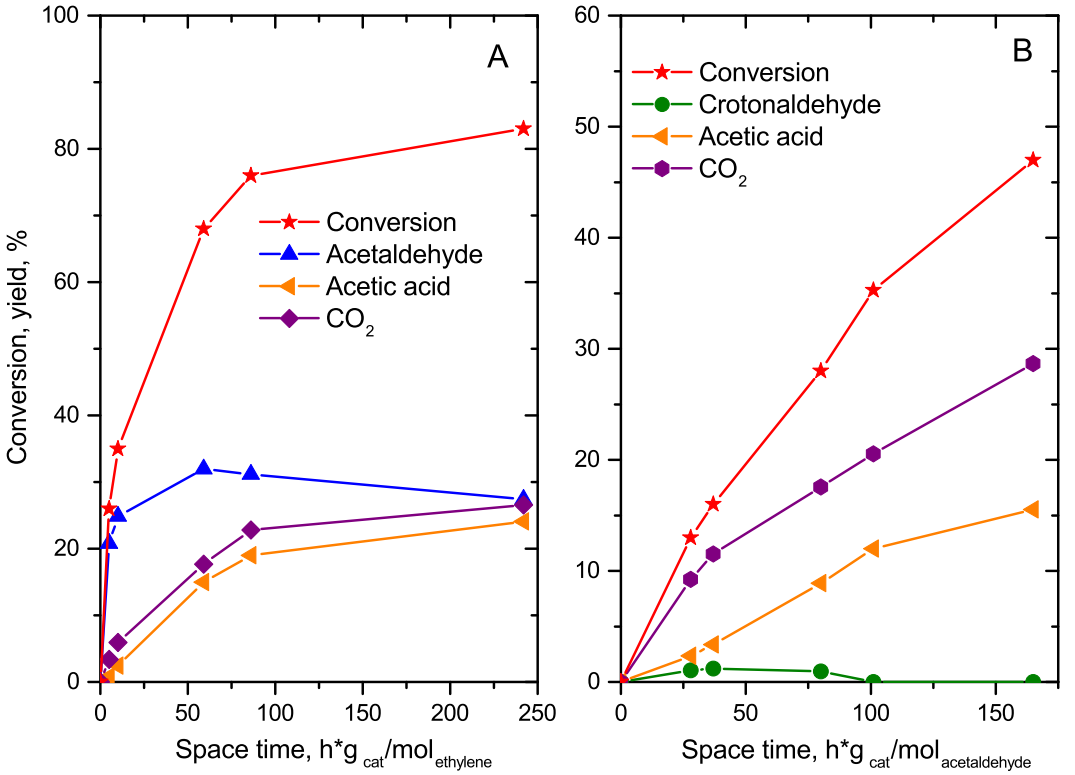

Fig. 9

Fig. 10. Effect of temperature in selective oxidation of ethylene over catalysts with different vanadia loadings (A) 0.4Pd2.2V (B) 0.4Pd4.6V (C) 0.4Pd8.6V. The space time was 205 g_{cat}. $mol^{-1}_{ethylene}$. The partial pressures of ethylene, oxygen and water were the same as those given in the legend of Fig. 7.

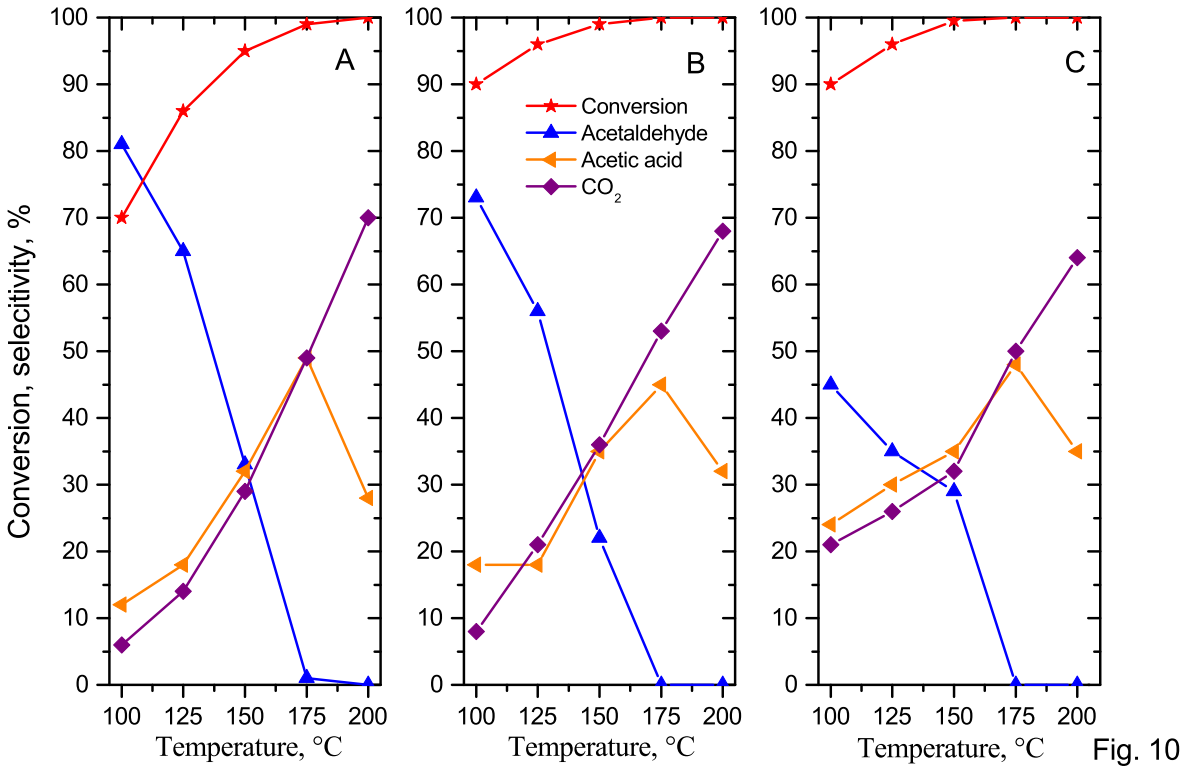

Fig. 11. Effect of temperature on the selective oxidation of (A)ethylene, (B) acetaldehyde and (C) acetic acid over 0.4Pd4.6V catalyst. The space time for ethylene was 205 h g_{cat}. $mol^{-1}_{reactant}$ and for aceteldhyde or acetic acid was 410 h g_{cat}. $mol^{-1}_{reactant}$. The partial pressures of ethylene and acetaldehyde or acetic acid were 3.4 and 1.7 kPa, respectively.

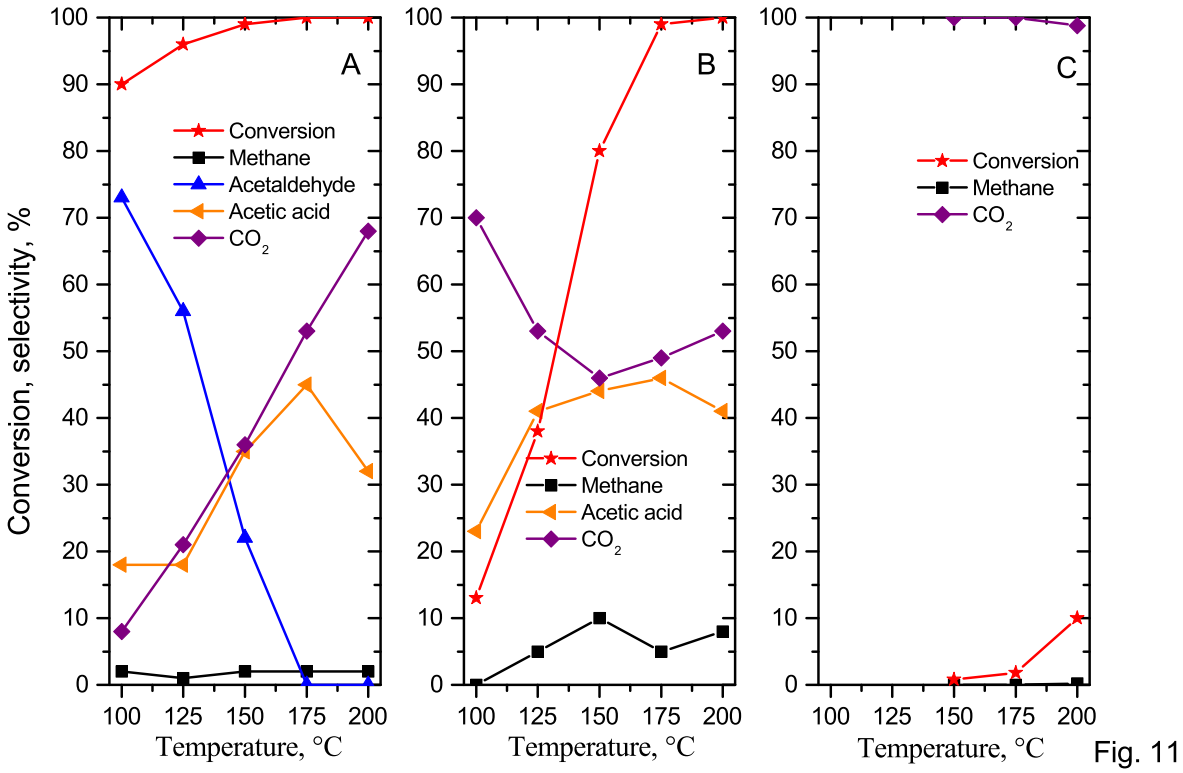

Fig. 11

Table 1. Specific surface area and active phase composition of titania-supported catalysts.

Catalyst[a]	SSA, m^2/g	Pd content, wt %		V_2O_5 content, wt %	
		fresh	used	fresh	used
0.01Pd2.1V	n.m.[b]	n.d.[c]	n.d.[c]	2.84	n. m[b]
0.1Pd2.1V	n.m.[b]	0.11	n.m.[b]	2.26	2.34
0.4Pd2.1V	55	0.40	0.39	2.18	2.16
0.4Pd4.2V	53	0.37	0.39	4.59	4.56
0.4Pd8.4V	50	0.42	0.38	8.57	8.40

[a] In the designation of the Pd-containing V_2O_5/TiO_2 samples V stands for V_2O_5/TiO_2 the number before the letter symbols gives the Pd and V content of the catalyst in weight percent.[b]Not measured. [c] Non detectable.

Table 2. Results of H_2-TPR measurements.

Catalyst	Low-temperature peak		High-temperature peak		$\sum H_2/V$
	H_2 (μmol g^{-1})	H_2/V	H_2 (μmol g^{-1})	H_2/V	
0.4Pd[a]	17	-	-	(0.46)[a]	-
2.2V	-	-	311	-	1.27
0.4Pd2.2V	-	-	120	0.49	0.49
4.6V	-	-	537	-	1,13
0.4Pd4.6V	91	0.18	163	0.32	0.50
8.6V	-	-	1114	-	1.17
0.4Pd8.6V	168; 306	0.18; 0.33	136	0.15	0.66

[a] Pd content of the sample is 0,39 wt% (38 μmol/g); H_2 consumption 17 μmol/g, i. e., $H_2/Pd = 0.46$